Quaternary Research 73 (2010) 385–392

Contents lists available at ScienceDirect

Quaternary Research

journal homepage: www.elsevier.com/locate/yqres

Late Quaternary climatic events and sea-level changes recorded by turbidite activity, Dakar Canyon, NW Africa

Roberto Pierau [a,*], Till J.J. Hanebuth [a], Sebastian Krastel [b], Rüdiger Henrich [a]

[a] MARUM — Center for Marine Environmental Sciences and Faculty of Geosciences, University of Bremen, Klagenfurter Straße, 28359 Bremen, Germany
[b] IFM Geomar, Wischhofstr. 1-3, 24148 Kiel, Germany

ARTICLE INFO

Article history:
Received 13 February 2008
Available online 27 November 2009

Keywords:
Turbidite system
Sea-level change
Palaeoclimate
NW Africa
Heinrich equivalents

ABSTRACT

The relationship of sea-level changes and short-term climatic changes with turbidite deposition is poorly documented, although the mechanisms of gravity-driven sediment transport in submarine canyons during sea-level changes have been reported from many regions. This study focuses on the activity of the Dakar Canyon off southern Senegal in response to major glacial/interglacial sea-level shifts and variability in the NW-African continental climate. The sedimentary record from the canyon allows us to determine the timing of turbidite events and, on the basis of XRF-scanning element data, we have identified the climate signal at a sub-millennial time scale from the surrounding hemipelagic sediments. Over the late Quaternary the highest frequency in turbidite activity in the Dakar Canyon is confined to major climatic terminations when remobilisation of sediments from the shelf was triggered by the eustatic sea-level rise. However, episodic turbidite events coincide with the timing of Heinrich events in the North Atlantic. During these times continental climate has changed rapidly, with evidence for higher dust supply over NW Africa which has fed turbidity currents. Increased aridity and enhanced wind strength in the southern Saharan–Sahelian zone may have provided a source for this dust.

Introduction

Submarine canyons play a major role as conduits for sediment transport from the continental shelf and upper slope into the deep-sea basins (Weaver et al., 2000). Several canyons that incise the passive NW-African continental margin have been investigated in terms of their general sedimentation processes (Seibold and Fütterer, 1982; Zühlsdorff et al., 2007). These studies have postulated a major influence of glacial/interglacial sea-level changes and climatic variability on the continental sediment supply. The Quaternary climate history of NW-Africa has been reconstructed from marine and terrestrial archives and suggests significant climate change from arid glacial condition to a more humid climate during the early Holocene (Sarnthein et al., 1982; Rognon and Coudé-Gaussen, 1996; deMenocal et al., 2000a; Kuhlmann et al., 2004). In contrast, the control of sub-millennial climatic changes on sediment dynamics is poorly known in the subtropical North Atlantic realm. In this study we reconstruct the late Quaternary turbidite history of the Dakar Canyon to unravel these sedimentation controlling factors based on a high-resolution age model. We discuss the sedimentary imprints of the interplay between sea level and climatic changes, and their potential to trigger turbidity currents.

Study area

The cold southward directed Canary Current, as a part of the Eastern Boundary Current System, is the major surface current along the NW-African margin (Mittelstaedt, 1991). The surface water masses in the subtropical North Atlantic south of 20°N are dominated by a wind-driven subtropical gyre (Stramma et al., 2005). These surface currents are underlain by the South Atlantic Central Water and the North Atlantic Central Water (Lonsdale, 1982). Deep-water currents are represented by the North Atlantic Deep Water at depths between 1200–4000 m (Stramma and Schott, 1999) and the Antarctic Bottom Water (AABW) below a water depth of 4000 m (Wynn et al., 2000).

The seasonal migration of the Intertropical Convergence Zone (ITCZ) is the most important atmospheric feature in NW Africa (Nicholson, 2000). During boreal summer, the northward shift of the ITCZ (20°N during August) is accompanied by the humid "SW" monsoon south of the ITCZ. Northeast directed trade winds prevail during winter times when the ITCZ has migrated to the southward position of 5°N. The trade winds and the overlying Sahara Air Layer are the prevailing wind systems over NW Africa (Fig. 1a) and drive

* Corresponding author. PanTerra Geoconsultants B.V., Weversbaan 1-3, 2352BZ Leiderdorp, The Netherlands. Fax: +31 71 301 0802.
E-mail address: r.pierau@panterra.nl (R. Pierau).

0033-5894/$ – see front matter
doi:10.1016/j.yqres.2009.07.010

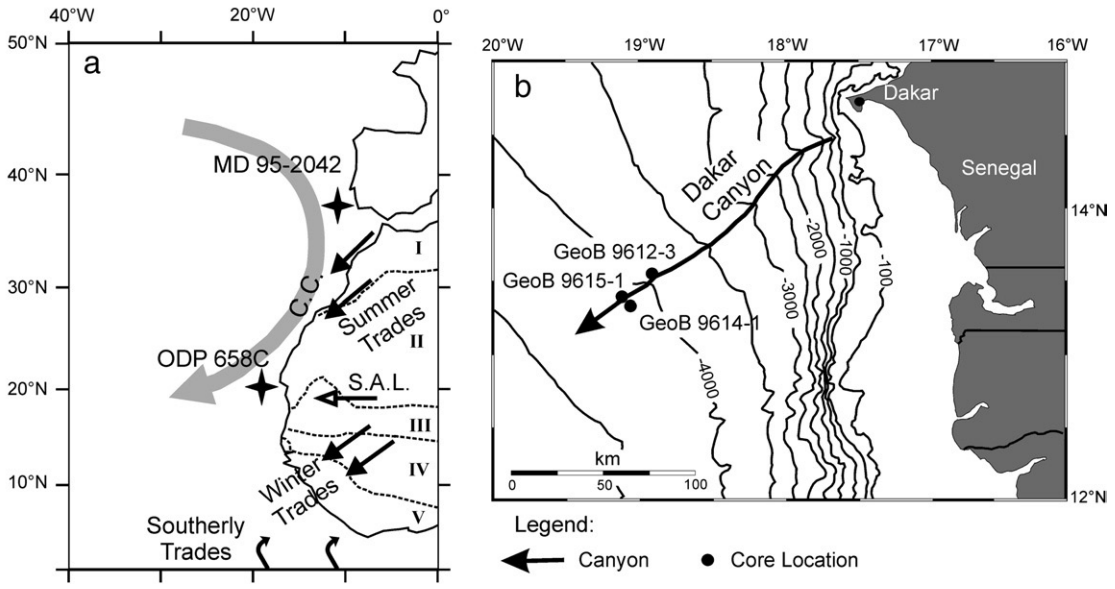

Figure 1. Map of the Dakar Canyon and surrounding area. (a) Overview of the study area including the major surface current (C.C. — Canary Current), the prevailing wind systems (S.A.L. — Sahara Air Layer and trade wind system) and the major vegetation zones of NW-Africa (modified after Hooghiemstra et al., 2006, I — Mediterranean vegetation, II — Saharan desert, III — Sahelian vegetation, IV — Sudanian savannah, V — Guinean rain forest). (b) Map of the Dakar Canyon including the locations of the presented cores. Bathymetry is taken from GEBCO.

major dust transport from the Sahara–Sahelian zone towards the Atlantic Ocean (Koopmann, 1981; Prospero and Lamb, 2003). Fluvial supply in the study area is restricted to the Senegal River north of Dakar but plays only a minor role in sediment supply (Redois and Debenay, 1999). Therefore, the surface sediments on the Senegalese shelf consist of quartz sands and carbonate shell fragments (McMaster and Lachance, 1969; Barusseau et al., 1988; Redois and Debenay, 1999). These sands have originated from palaeo-dunes that, in turn, have formed around the last glacial maximum (LGM) as a result of increased aridity and wind strength (Sarnthein and Diester-Haass, 1977; Lancaster et al., 2002), and low sea level providing widely exposed shelf areas. The Senegalese Shelf varies in width between 50–100 km (Hagen, 2001) and the average depth of the shelf break south of 15°N is found in about 100–150 m present water depths (McMaster and Lachance, 1969).

Along the Iberian and NW-African margin the sea surface temperatures (SST) show a range from about 18°C during the Late Glacial period to 21.5°C during early Holocene times, indicating a considerable southward transport of cooler subpolar water masses by the Canary Current (Zhao et al., 1995). Furthermore, cooler SST could also be attributed to enhanced upwelling forced by stronger trade wind intensity (Martinez et al., 1999). Consequently, the inflow of cold surface water masses along the NW-African margin coincides with low orbital boreal summer insolation and is thought to have additionally influenced the regional atmospheric and climate pattern of NW-Africa (deMenocal et al., 2000b). As a result,

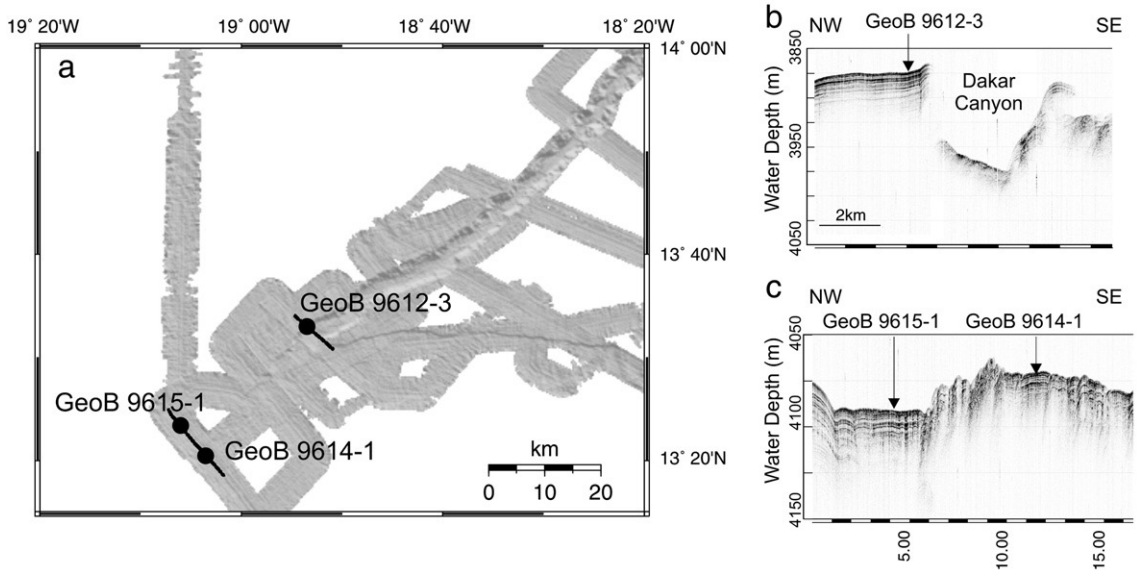

Figure 2. Bathymetric multibeam map of the distal Dakar Canyon (a) including the core locations. The locations of the seismic profiles are shown as black lines. (b and c) Narrow beam sediment echo sounder profile crossing the location of Cores 9612-3, 9615-1 and 9614-1. The distance in altitude between the canyon bottom and the top of the levee as depicted in (b) is about 100 m.

Table 1
Key parameters of cores investigated in this study including core number, geographic position and water depth.

Core number	Latitude	Longitude	Water depth (m)
GeoB 9612-3	13° 33.01′ N	18° 53.50′ W	3893
GeoB 9614-1	13° 20.54′ N	19° 03.56′ W	4090
GeoB 9615-1	13° 23.68′ N	19° 06.27′ W	4180

Table 2
AMS radiocarbon dating and calibrated ages of Core 9612-3.

Core depth (cm)	Lab ID	^{14}C yr BP ± a	Calib. age, two sigma range (cal yr BP)	Calib. age (cal ka BP)
55	KIA30490	12650 ± 90	13860–14610	14.1
68	KIA30506	13380 ± 80	15030–15690	15.3
111	KIA30488	18400 ± 140	20810–21910	21.3
133	KIA30487	29530 ± 480/−450		34.5

due to the arid glacial conditions and intensified trade winds, a period of active dune formation occurred between 25 and 14.8 ka in the western Sahara (Sarnthein, 1978; Lancaster et al., 2002). During the LGM sea-level lowstand the exposed shelf south of Dakar was also covered by dune fields, whose remnants can still be traced on the shelf today (Barusseau et al., 1988).

Materials and dating methods

The bathymetry and architecture of the Dakar Canyon (Fig. 2a) were mapped using a bathymetric multibeam system and a sediment echosounder. At the upper slope the canyon incises vertically up to 700 m into the strata and is up to ~10 km wide. The canyon cuts straight downslope and the incision depths of the canyon decrease basinwards down to less than ~20 m at the continental rise in ~4000 m water depth. Irregular high-amplitude reflectors indicate a sandy infill of the canyon's thalweg (Figs. 2b, c). At the distal part the canyon splits into a main active channel and a parallel channel remnant.

This study focuses on three gravity cores recovered from the thalweg (GeoB 9614-1 and GeoB 9615-1) and its northern levee in the direct vicinity of the canyon (GeoB 9612-3, Fig. 1b, Table 1). The sedimentary records of all these cores consist of hemipelagic sediments composed of silty mud, which are frequently intercalated by fine sandy and silty turbidite beds at distinct intervals. The exact differentiation between hemipelagites and turbidites was determined by visual core description and X-ray radiographies, which were performed on 1 cm thick sediment slides. At the northern levee of the canyon the hydroacoustic profile depicts well-stratified deposits (Fig. 2b) as identified as hemipelagic sediments in Core 9612-3. The turbidites in this core are of spill-over origin and according to the X-ray radiographies the hemipelagic sediments show no erosional features. Thus this core was selected to provide a suitable stratigraphical model which can be transferred as a reference to the other investigated cores.

The planktonic foraminifera *Globigerinoides ruber* (white) was used for δ^{18}O stable isotope measurements and the planktonic foraminifers *G. ruber* (w/p), *G. sacculifer* and *Orbulina universa* were collected for accelerator mass spectrometry radiocarbon (AMS) dating at the Leibniz Laboratory for Radiocarbon Dating and Isotope Research in Kiel, Germany. The elements Ca and Ti were measured in 1 cm resolution using a non-destructive X-ray Fluorescence (XRF) Core Scanner.

The age model for Core 9612-3 is based on its stable oxygen isotope curve (Fig. 3) which is correlated to the orbitally tuned SPECMAP record (Martinson et al., 1987). Four radiocarbon dates are used to improve the age model for the younger part of the record (Table 2). A standard reservoir age of 400 yr is assumed for calibration regarding to short-lasting period of winter upwelling. The radiocarbon ages younger than 24 ^{14}C ka BP were corrected and calibrated using CALIB REV5.0.1 (Stuiver et al., 1998). Older radiocarbon ages were calibrated using the function of Bard et al. (1998). All radiocarbon ages are given in calibrated thousands of years before present in the following (cal ka BP).

Results

In this paper we focus on the occurrence of turbidites in the Dakar Canyon during the late Quaternary. Thickness of the turbidites varies from a few centimetres (minimum 1 cm) to a comparably thick turbidite of 135 cm in Core 9615-1 (Fig. 4, Table 3). According to the analysis of the X-ray radiographies all turbidites show a clear fining-upward sequence and consist mostly of cross-laminated fine sands overlain by laminated silts and homogenous mud. The cores recovered in the canyon axis consist of relatively thick turbidites

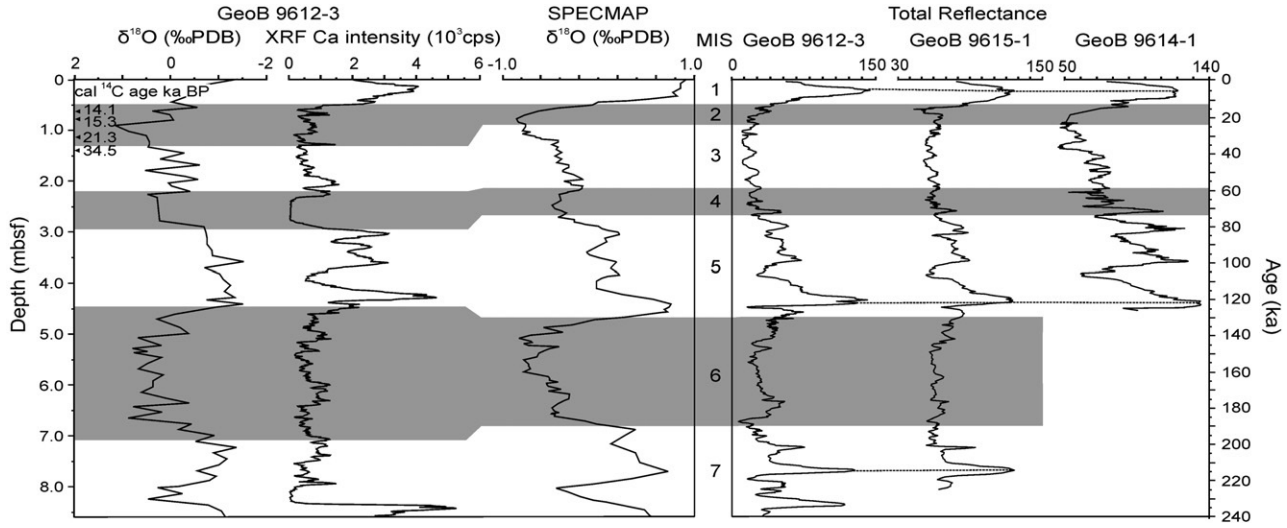

Figure 3. Oxygen isotope record and XRF Ca intensity of Core 9612-3 against core depth (mbsf — metres below seafloor) compared to the SPECMAP record. The shaded areas indicate glacial marine oxygen isotope stages. Cores 9614-1 and 9615-1 were correlated with 9612-3 by their characteristic total reflectance pattern of the hemipelagites (dotted lines). Turbidites were cut out of these records.

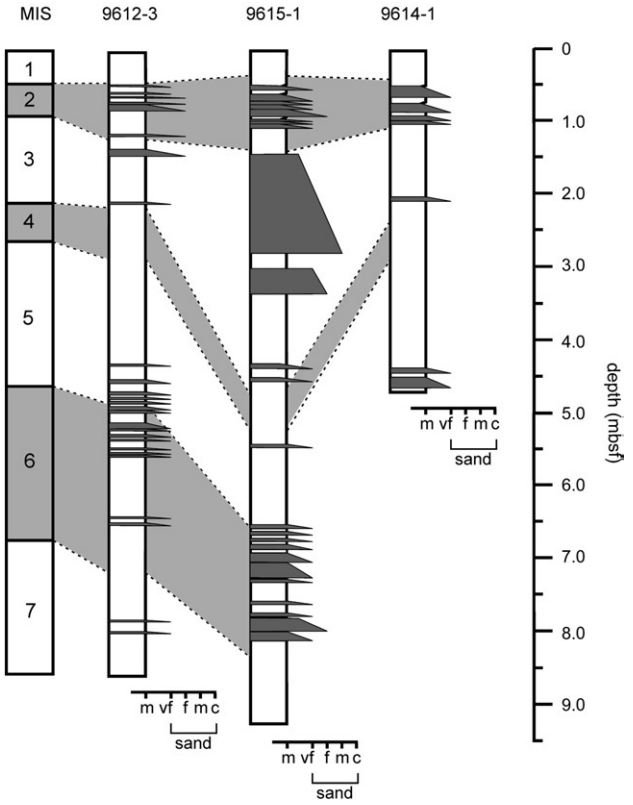

Figure 4. Schematic sedimentary columns of Cores 9612-3, 9615-1 and 9614-1 against age and depths (mbsf). The grain size distribution of the turbidites is expressed in mud (m) and sand content (vf — very fine, f — fine, m — medium, c — coarse).

(Table 3) with coarse sandy material at their base. The T_A and T_B units as parts of the lower Bouma-Sequence (Bouma, 1962) are only partly preserved. The fine-grained deposits, reflected in the T_C to T_D units, occur in most of the turbidites. This fine material was deposited a) as spill-over turbidites in the levee Core 9612-3 and b) as fine sediment suspension in the canyon axis. The top sections of the turbidites are often destroyed by intensive bioturbation. Therefore, it is partly problematic to distinguish a turbidite top from the overlying hemipelagic sediments. In such a case the beginning of the hemipelagic sedimentation was defined by increased numbers of foraminifers (Zühlsdorff et al., 2007).

To determine the age of the cores we subtracted the turbidite sections from all records, receiving a continuous hemipelagic sedimentation succession, and correlated the two other investigated cores (9615-1 and 9614-1) by their characteristic total reflectance pattern (Fig. 3). Ages of turbidites are considered to be equivalent to the age derived for the onset of hemipelagic sedimentation on the top of the relevant turbidite. Based on core correlation and age determination of the turbidites, we combined the turbidite records of all three cores to provide a stacked turbidite sequence for the Dakar Canyon. This stacked record consists in total of 40 individual turbidite beds (Table 3).

The highest turbidite frequency is recorded during the two past glacial/interglacial transitions, and thus coincides with the respective rise in the eustatic sea level (Fig. 5a). For Termination I (T1, 15.7–13.9 cal ka BP) five events/ka have occurred whereas a lower frequency of 1.2 events/ka is recorded for Termination II (T2, 137.2–125.2 ka). Furthermore, turbidites that are concentrated around these terminations show the highest thickness (Fig. 4). In addition, some thin turbidites occur around 60, 49, 28 and 23 ka as well as prior to T2 (at 220, 170 and 164 ka, Fig. 5a), which could not have been triggered by major rises in sea level. These events coincide, however, with lower SST (Figs. 5b, c) along the Iberian and NW-African continental margin (Zhao et al., 1995; Pailler and Bard, 2002) and coeval with the timing of Heinrich events in the North Atlantic (Thouveney et al., 2000; Moreno et al., 2002). Furthermore, higher Ti/Ca ratios (Fig. 5d) are recorded in the hemipelagites in Core 9612-3 during these Heinrich equivalent time intervals (HE). The marine carbonate content is reflected by the XRF Ca intensity, whereas Ti is related to siliciclastic components of terrigenous origin. The Ti/Ca ratio is, therefore, commonly used as a proxy for the influx of terrigenous material in marine sediments (Arz et al., 1998). Due to the absence of riverine input in the study area, this ratio reflects here the variability of dust input from the continent.

Two episodes of very high Ti/Ca ratios (Fig. 5d) and extremely low XRF Ca intensities (Fig. 3) are observed around 220 and 70 ka in Core 9612-3. This core was recovered in a water depth of 3900 m and could be influenced by depth changes of the carbonate unsaturated AABW (Sarnthein et al., 1982) which, in turn, would lead to carbonate solution in the sediment. According to this effect, low Ca values led to irregularly high values of the Ti/Ca ratio.

Discussion

Both continental climatic changes and sea-level oscillations controlled the turbidite activity in the Dakar Canyon. During T1 the steadily rising sea level (Peltier and Fairbanks, 2006), due to the melting of the Northern Hemisphere ice sheets, was interrupted by one or more short time intervals of very rapid rises known as meltwater pulses (MWP, Fairbanks, 1989, Hanebuth et al., 2000). The interval of very high turbidite activity during T1 partly coincides with MWP1A (14.6–14.3 cal ka BP, Fig. 6) when the sea level rose as much as 15 m within a few centuries (Hanebuth et al., 2000). Furthermore, a high Ti/Ca ratio is recorded at 15 cal ka BP that fits with the timing of Heinrich event 1 in the North Atlantic (Fig. 6). This period coevals with generally dry conditions over the NW-African continent (Lèzine, 1991). Contemporaneously, a weakened thermohaline circulation led to a stronger hemispheric temperature gradient coupled with intensified trade winds (Vidal et al., 1997; Jullien et al., 2007). The resulting southward shift of the ITCZ (Jennerjahn et al., 2004) has reduced the monsoonal precipitation over NW-Africa (deMenocal et al., 2000a) and led to a southward migration of the vegetation zones (Hooghiemstra et al., 2006). In general, the aeolian dust input off NW-Africa was significantly higher during glacial periods (Matthewson et al., 1995; Moreno et al., 2001). The Ti/Ca ratio of Core 9612-3 supports this observation, reflected by higher Ti/Ca ratios during periods of enhanced dust supply (Fig. 6). Furthermore, along NW-Africa, the river discharge during the LGM was nearly not existent due to the arid climate conditions (Barusseau et al., 1988).

Enhanced climate-induced dust supply towards the exposed shelf and active dune formation between 16 and 14 cal ka BP as well as during the Younger Dryas at 12.6 cal ka BP (Sarnthein, 1978; Lancaster et al., 2002) have provided a considerable sediment source for gravity-driven mass flows off the shelf break. The dune fields have formed at the lee side of the tectonic high of Ndiass horst, east of Dakar, and extended parallel to the former coastline (Barusseau et al., 1988). These dune remnants are obviously found on the entire modern shelf up to a water depth of 20 m and have even been discovered close to the shelf break in 120 m modern water depth (Barusseau et al., 1988). The loose sands of these dunes were probably very efficiently remobilised during the subsequent rapid transgression and their material was collected by and transported downslope through the canyon. The large volume of reworked sediments is expressed in massive thickness and high frequency of turbidite deposition during T1 (Fig. 4). The interaction of these climatically controlled sediment supply onto the exposed shelf and the following

Table 3
Age, thickness and Bouma Units of the turbidites in Cores 9612-3, 9614-1, and 9615-1 and the stacked turbidite record of the Dakar Canyon.

GeoB 9612-3			GeoB 9615-1			GeoB 9614-1			Stacked turbidite record	
Age (ka)	Thickness (cm)	Bouma Unit	Age (ka)	Thickness (cm)	Bouma Unit	Age (ka)	Thickness (cm)	Bouma Unit	Turbidite No.	Age (ka)
12.3	1	?	14.3	6	T_B–T_C	14.7	8	T_C–T_E	1	12.3
13.9	4	T_C	**xx**	1	T_B	18.2	17	T_A–T_B	2	13.9
14.6	2	?	15.1	14	T_B–T_E	22.4	15	T_B–T_E	3	14.3
14.8	2	T_C	15.3	6	T_B–T_E	23.2	13	T_C	4	14.6/14.7
14.9	11	T_B–T_C	**xx**	8	T_C–T_E	48.8	5	T_C	5	14.8
22.1	3	?	15.4	5	T_C–T_E	123.9	8	T_C	6	14.9/15.1
29.3	10	T_A–T_D	**xx**	2	T_C	125.2	20	T_B–T_E	7	15.3
57.2	4	?	15.5	5	T_C				8	15.4
125.5	3	?	15.7	4	?				9	15.5
127.6	3	T_C	**xx**	3	T_C				10	15.7
xx	5	T_C	24.2	135	T_A–T_C				11	18.2
128.2	2	?	28.5	38	T_B–T_C				12	22.1/22.4
128.3	4	?	57.2	6	T_C–T_E				13	23.2
128.7	3	?	60.2	5	?				14	24.2
129.3	5	T_C	82.9	4	?				15	28.5/29.3
129.6	3	T_C	131.6	4	T_D				16	48.8
132.9	9	T_B–T_C	132.3	4	T_D				17	57.2
xx	3	?	136.5	5	T_C–T_D				18	60.2
133.6	3	?	137.2	10	T_C–T_D				19	82.9
134.0	4	T_C–T_D	**xx**	16	?				20	125.2
135.0	5	?	141.3	21	T_A–T_C				21	125.5/125.2
136.3	2	?	**xx**	7	T_C–T_E				22	127.6
xx	3	?	xx	3	T_C				23	128.2
170.3	2	?	163.8	3	?				24	128.3
173.7	4	?	171.7	21	T_B–T_E				25	128.7
216.7	3	?	173.3	15	T_B–T_E				26	129.3
219.7	8	T_C							27	129.6
									28	131.6
									29	132.3/132.9
									30	133.6
									31	134.0
									32	135.0
									33	136.3/136.5
									34	137.2
									35	141.3
									36	163.8
									37	170.3/171.7
									38	173.3/173.7
									39	216.7
									40	219.7

Columns marked by **xx** consist of turbidites without age determination due to the direct covering of two individual turbidites. Bouma Units which are marked with ? were not clearly identified.

rapid transgression were responsible for the high turbidite occurrence during the T1.

A low Ti/Ca ratio after 14 cal ka BP displays the onset of the African Humid Period (14.8 cal ka BP) when the climate has changed rapidly towards humid conditions (deMenocal et al., 2000a). The latest turbidite bed coincides remarkably with a short interruption of this wet period by the arid Younger Dryas (Gasse et al., 1989) which was centred around 12.6 cal ka BP (Fig. 6, deMenocal et al., 2000a). Comparably, humid conditions and the general sea-level stability have prevented further turbidity activity during the Holocene (Fig. 5a).

The results can be transferred to the much less understood Termination II. During this climatic transition two phases of increased turbidite activity are recorded at 136–132 ka and at 130–128 ka (Fig. 6). Moreover, two turbidite events have occurred in the time interval from 126–122 ka. High Ti/Ca ratios occur around 138 ka in Core 9612-3. Elevated Ti/Ca ratios are also detected during these two phases of high turbidite activity and coincide with decreases in SST recorded in Core MD95-2042 (Fig. 6, Pailler and Bard, 2002). In general, we assume a comparable situation for the turbidite depositional history during T2 as described for T1. The sea-level history during T2 was possibly characterized by an early, temporary highstand (ca. 134 ka) at intermediate levels, followed by a fall in sea level with a subsequently stable period at 133–130 ka and finally by the ultimate sea-level rise into the marine oxygen isotope stage (MIS) 5e (Siddall et al., 2006).

The frequent turbidite activity, that has started around 136 ka, coincides with the initiation of the early sea-level rise (Fig. 6). No activity is recorded during the succeeding phase of sea-level stagnation whereas a second period of high turbidite deposition occurred contemporaneous with the second interval of sea-level rise. A relatively high Ti/Ca ratio is registered prior to the early sea-level rise (Fig. 6), which indicates an episode of enhanced dust supply. Dune fields have probably formed on the exposed shelf prior to T2 as well. Subsequently, during rapid sea-level rise, the dunes may have been eroded and the material was transported trough the canyon by turbidity currents as observed as an efficient mechanism during T1. The low Ti/Ca ratio through MIS 5 (Fig. 5d) probably indicates more humid conditions and less dust supply. This reduced dust input and a high sea level might have impeded further turbidite activity.

Sporadically appearing turbidites are recorded during MIS 6 and MIS 3 (Fig. 5a). These turbidites consist of laminated fine-grained sediments. They are, in general, thinner and finer than those turbidites that have deposited during the two major climate transitions (Fig. 7). The ages of these turbidites coincide with HE (Fig. 5a). The occurrence of HE is associated with significant peaks

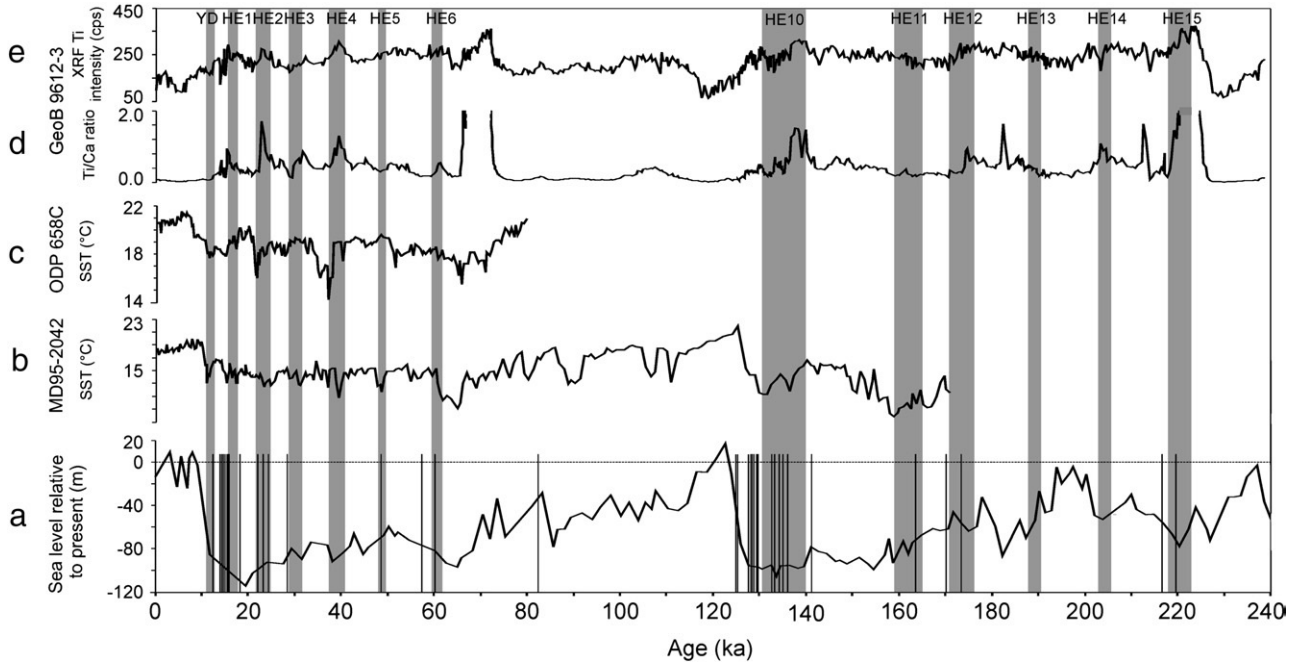

Figure 5. Comparison of the 9612-3 sediment record with regional and global climate proxy data. (a) illustrates the stacked turbidite record (each black bar indicates a single turbidite event) of the Dakar Canyon in relation to the global sea-level curve (Siddall et al., 2003). Abrupt drops in SST (b, c) of MD95-2042 (Pailler and Bard, 2002) and ODP 658C (Zhao et al., 1995) demonstrate the influence of cold surface water along the Portuguese and NW-African continental margin during HE (marked in grey). The changes of Ti/Ca ratio of Core 9612-3 and XRF Ti intensity (d, e) coeval with HE and show synchronous millennial-scale oscillations with shifts in SST of Cores MD95-2042 and ODP 658C.

in the Ti/Ca ratio of Core 9612-3 (Fig. 5d) and is accompanied by intervals of low SST as recorded in the Cores MD95-2042 and ODP 658C (Zhao et al., 1995; Pailler and Bard, 2002). These observations seem to indicate episodes of short-term climatic changes in the hinterland influencing the seaward flux of dust. Jullien et al. (2007) argue that a southward shift of the ITCZ reorganises the atmospheric pattern of NW-Africa which results in arid conditions in the hinterland with enhanced trade wind intensity. During HE sea-level oscillations have also occurred but surely at significantly lower amplitudes than during major climate terminations (Lambeck et al., 2002). During these times, sea level was 60–90 m lower than present (Yokoyama et al., 2001). The shelf was partly exposed and these arid episodes were probably responsible for the deposition of dust and the enhanced sediment accumulation on the shelf. Slightly rising sea level during these HE could have remobilised dust from the shelf. According to the detailed sea-level reconstruction of coral terraces from the Huon Peninsula during these HEs, sea level rose rapidly towards the end of an HE (Yokoyama et al., 2001). We

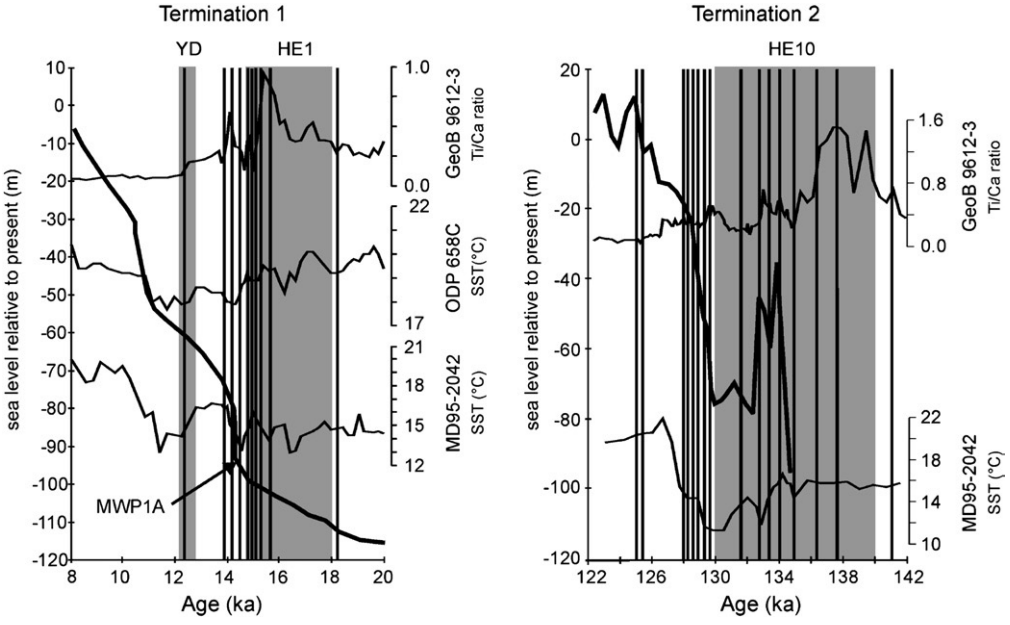

Figure 6. Turbidite activity during T1 and T2 in the Dakar Canyon in comparison with sea-level change, SST and Ti/Ca ratio of Core 9612-3. The thick grey line indicates the sea level and the grey marked areas illustrate periods of short-term climatic changes. Each black bar represents a single turbidite. The highest activity of turbidite deposition during both terminations correlates well with episodes of rapid sea-level rise.

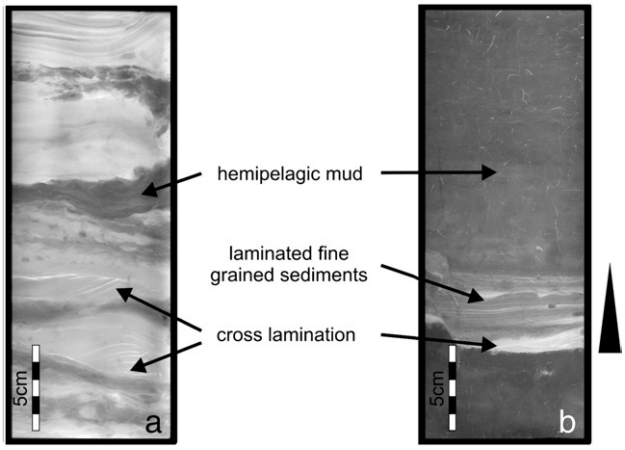

Figure 7. X-ray radiographs of Core 9615-1 showing different sedimentary structures of turbidites. (a) 75–100 cm core depths display a sector of frequent turbidite deposition during Termination I. The turbidites consists of relative thick and coarse sediments. (b) 425–450 cm core depths show a thin fining-upward turbidite sequence deposited during a Heinrich time equivalent.

conclude that during HEs dust was deposited on the shelf which was subsequently remobilised at the termination of an HE recorded in the turbidite activity.

Conclusions

Two main phases of turbidite activity coinciding with the past two glacial terminations are identified in the Dakar Canyon. They are linked to major climatic transitions in association with rapidly rising eustatic sea level. The turbidite activity during these terminations was triggered by the remobilisation of sediments which had previously been deposited on the exposed shelf in the form of aeolian dunes under arid glacial climate conditions and an intensified trade wind regime. The significant influence of MWP1A is detectable by an exceptional high turbidite activity. The dynamic of turbidite activity during Termination II seems to reinforce the recent progress in sea-level reconstructions. The onset of humid conditions after major climate terminations has coincided with a die-off of turbidite activity probably due to reduced dust supply. High and relatively stable sea levels during MIS 5 and the Holocene have additionally impeded further turbidite activity.

The short-lasting climatic changes during HE are characterized by reduced monsoon intensity and southward migration of the vegetation zones resulting in enhanced dust flux. Increases in the Ti/Ca ratios indicate a higher aeolian input and coeval with the deposition of turbidites. This observation probably shows that the influence of HE extended as far south as into the study area resulting in a large-scale reorganisation of the atmospheric and climatic pattern.

This study points out the potential of sedimentary canyon records as archives to reconstruct the interplay of even short-lasting climatic episodes and global sea-level oscillations considering the turbidite history.

Acknowledgments

The captain, crew, and shipboard participants of cruise M65/2 are thanked for their assistance. We also thank D.J.W. Piper and N. Lancaster for manuscript review and discussion. Swantje Boeschen, Brit Kockisch and Helga Heilmann are acknowledged for laboratory assistance. We also thank Christine Zühlsdorff, Dave Heslop, Ulrike Proske and Helge Meggers for useful comments on an early version of the manuscript. This work was funded through DFG-Research Center/Excellence Cluster "The Ocean in the Earth System."

References

Arz, H.W., Pätzold, J., Wefer, G., 1998. Correlated millennial-scale changes in surface hydrography and terrigenous sediment yield inferred from last-glacial marine deposits off Northeastern Brazil. Quaternary Research 50, 157–166.

Bard, E., Arnold, M., Hamelin, B., Tisnerat-Laborde, N., Cabioch, G., 1998. Radiocarbon calibration by means of mass spectrometric 230Th/234U and ^{14}C ages of corals. An updated data base including samples from Barbados, Mururoa and Tahiti. Radiocarbon 40, 1041–1085.

Barusseau, J.P., Giresse, P., Faure, H., Lezinet, A.M., Masse, J.P., 1988. Marine sedimentary environments on some parts of the tropical and equatorial Atlantic margins of Africa during the Late Quaternary. Continental Shelf Research 8, 1–21.

Bouma, A.H., 1962. Sedimentology of Some Flysch Deposits: A Graphic Approach to Facies Interpretation. Elsevier, Amsterdam.

deMenocal, P., Ortiz, J., Guilderson, T., Adkins, J., Sarnthein, M., Baker, L., Yarusinsky, M., 2000a. Abrupt onset and termination of the African Humid Period: rapid climate response to gradual insolation forcing. Quaternary Science Review 19, 347–361.

deMenocal, P.B., Ortiz, J., Guilderson, T., Sarnthein, M., 2000b. Coherent high- and low-latitude climate variability during the Holocene Warm Period. Science 288, 2198–2202.

Fairbanks, R.G., 1989. A 17,000 year glacial eustatic sea level record: influence of glacial melting rates on the Younger Dryas event and deep ocean circulation. Nature 342, 637–641.

Gasse, F., Lédée, V., Massault, M., Fontes, J.-C., 1989. Water-level fluctuations of Lake Tanganyika in phase with oceanic changes during the last glaciation and deglaciation. Nature 342, 57–59.

Hagen, E., 2001. Northwest African upwelling scenario. Oceanologica 24, 113–128.

Hanebuth, T., Stattergger, K., Grootes, P.M., 2000. Rapid flooding of the Sunda Shelf: a late-glacial sea-level record. Science 288, 1033–1035.

Hooghiemstra, H., Lézine, A.-M., Leroy, S.A.G., Dupont, L., Marret, F., 2006. Late Quaternary palynology in marine sediments: a synthesis of the understanding of pollen distribution patterns in the NW African setting. Quaternary International 148, 29–44.

Jennerjahn, T.C., Ittekkot, V., Arz, H.W., Behling, H., Pätzold, J., Wefer, G., 2004. Asynchronous terrestrial and marine signals of climate change during Heinrich Events. Science 306, 2236–2239.

Jullien, E., Grousset, F., Malaizé, B., Duprat, J., Sanchez-Goni, M.F., Eynaud, F., Charlier, K., Schneider, R., Bory, A., Bout, V., Flores, J.A., 2007. Low-latitude "dusty events" vs. high-latitude "icy Heinrich events". Quaternary Research 68, 379–386.

Koopmann, B., 1981. Sedimentation von Saharastaub im subtropischen Nordaltantik während der letzten 25.000Jahre. Meteor Forschungs-Ergebnisse 35, 23–59.

Kuhlmann, H., Meggers, H., Freudenthal, T., Wefer, G., 2004. The transition of the monsoonal and the N Atlantic climate system off NW Africa during the Holocene. Geophysical Research Letters 31.

Lambeck, K., Esat, T.M., Potter, E.-K., 2002. Links between climate and sea levels for the past three million years. Nature 419, 199–206.

Lancaster, N., Kocurek, G., Singhvi, A., Pandey, V., Deynoux, M., Ghienne, J.-F., Lô, K., 2002. Late Pleistocene and Holocene dune activity and wind regimes in the western Sahara Desert of Mauritania. Geology 30, 991–994.

Lèzine, A.-M., 1991. West African paleoclimates during the last climatic cycle inferred from an Atlantic deep-sea pollen record. Quaternary International 35, 456–463.

Lonsdale, P., 1982. Sediment drift of the Northeast Atlantic and their relationship to the observed abyssal currents. Bulletin de l'Institut de Geologie du Bassin d'Aquitaine 141–150.

Martinez, P., Bertrand, P., Shimmield, G.B., Cochrane, K., Jorissen, F.J., Dignan, M., 1999. Upwelling intensity and ocean productivity changes off Cape Blanc (northwest Africa) during the last 70.000 years: geochemical and micropalaeontological evidence. Marine Geology 158.

Martinson, D.G., Pisias, N.G., Hays, J.D., Imbrie, J.D., Moore, T.C., Shackleton, N.J., 1987. Age dating and the orbital theory of the ice ages: development of a high-resolution 0 to 300,000-year chronostratigraphy. Quaternary Research 27, 1–29.

Matthewson, A.P., Shimmield, G.B., Kroon, D., 1995. A 300 kyr high-resolution aridity record of the North African continent. Paleoceanography 10, 677–692.

McMaster, R.L., Lachance, T.P., 1969. Northwestern African continental shelf sediments. Marine Geology 7, 57–67.

Mittelstaedt, E., 1991. The ocean boundary along the North-west African coast: circulation and oceanographic properties at the sea surface. Progress in Oceanography 26, 307–355.

Moreno, A., Targarona, J., Henderiks, J., Canals, M., Freudenthal, T., Meggers, H., 2001. Orbital forcing of dust supply to the North Canary Basin over the last 250 kyr. Quaternary Science Review 20, 1327–1339.

Moreno, E., Thouveny, N., Delanghe, D., McCave, I.N., Shackelton, N.J., 2002. Climatic and oceanographic changes in the Northeast Atlantic reflected by magnetic properties of sediments deposited on the Portuguese Margin during the last 340 ka. Earth and Planetary Science Letters 202, 465–480.

Nicholson, S.E., 2000. The nature of rainfall variability over Africa on time scales of decades to millenia. Global and Planetary Change 26, 137–158.

Pailler, D., Bard, E., 2002. High frequency palaeoceanographic changes during the past 140000 yr recorded by the organic matter in sediments of the Iberian Margin. Palaeogeographgy, Palaeoclimatology, Palaeoecology 181, 431–452.

Peltier, W.R., Fairbanks, R.G., 2006. Global glacial ice volume and Last Glacial Maximum

duration from an extended Barbados sea level record. Quaternary Science Review 25, 3322–3337.
Prospero, J.M., Lamb, P.J., 2003. African droughts and dust transport to the Caribbean: climate change implications. Science 302, 1024–1027.
Redois, F., Debenay, J.-P., 1999. Répartition des foraminifères benthiques actuels sur le plateau continental sénégalais au sud de Dakar. Oceanologica Acta 22, 215–232.
Rognon, P., Coudé-Gaussen, G., 1996. Paleoclimates off Northwest Africa (28°–35°N) about 18.00 yr B.P. based on continental eolian deposits. Quaternary Research 46, 118–126.
Sarnthein, M., 1978. Sand deserts during glacial maximum and climate optimum. Nature 272, 43–46.
Sarnthein, M., Diester-Haass, L., 1977. Eolian-sand turbidites. Journal of Sedimentary Petrology 47, 868–890.
Sarnthein, M., Thiede, J., Pflaumann, U., Erlenkeuser, H., Fütterer, D., Koopmann, B., Lange, H., Seibold, E., 1982. Atmospheric and Oceanic Circulation Patterns Off Northwest Africa during the past 25 Million Years. In: von Rad, U., Hinz, K., Sarnthein, M., Seibold, E. (Eds.), Geology of the Northwest African Continental Margin. Springer, Berlin, pp. 545–604.
Seibold, E., Fütterer, D., 1982. Sediment dynamics on the Northwest African continental margin. In: Scrutton, R.A., Talwabi, M. (Eds.), The Ocean Floor. John Wiley & Sons, Chichester, pp. 147–163.
Siddall, M., Bard, E., Rohling, E.J., Hemleben, C., 2006. Sea-level reversal during Termination II. Geology 34, 817–820.
Siddall, M., Rohling, E.J., Almogi-Labin, A., Hemleben, C., Meischer, D., Schmelzer, I., Smeed, D.A., 2003. Sea-level fluctuations during the last glacial cycle. Nature 423, 853–858.
Stramma, L., Hüttl, S., Schafstall, J., 2005. Water masses and currents in the upper tropical northeast Atlantic off northwest Africa. Journal of Geophysical Reserarch 110.
Stramma, L., Schott, F., 1999. The mean flow field of the tropical Atlantic Ocean. Deep-Sea Research II 46, 279–303.
Stuiver, M., Reimer, P.J., Bard, E., Beck, J.W., Burr, G.S., Hughen, K.A., Kromer, B., McCormac, G., Van der Plicht, J., Spurk, M., 1998. INTCAL98 radiocarbon age calibration, 24.000–0 cal BP. Radiocarbon 40, 1041–1084.
Thouveney, N., Moreno, E., Delanghe, D., Candon, L., Lancelot, Y., Shackelton, N.J., 2000. Rock magnetic detection of distal ice-rafted debris: clue for the identification of Heinrich events on the Portuguese margin. Earth and Planetary Science Letters 180, 61–75.
Vidal, L., Labeyrie, L., Cortijo, E., Arnold, M., Duplessy, J.C., Michel, E., Becqué, S., van Weering, T.C.E., 1997. Evidence for changes in the North Atlantic Deep Water linked to meltwater surges during the Heinrich events. Earth and Planetary Science Letters 146, 13–27.
Weaver, P.P.E., Wynn, R.B., Kenyon, N.H., Evans, J., 2000. Continental margin sedimentation, with special reference to the north-east Atlantic margin. Sedimentology 47, 239–356.
Wynn, R.B., Masson, D.G., Stow, D.A.V., Weaver, P.P.E., 2000. The Northwest African slope apron: a modern analogue for deep-water systems with complex seafloor topography. Marine and Petroleum Geology 17, 253–265.
Yokoyama, Y., Esat, T.M., Lambeck, K., 2001. Coupled climate and sea-level changes deduced from Huon Peninsula coral terraces of the last ice age. Earth and Planetary Science Letters 193, 579–587.
Zhao, M., Beveridge, N.A.S., Shackelton, N.J., Sarnthein, M., Eglinton, G., 1995. Molecular stratigraphy of cores off northwest Africa: Sea surface temperature history over the last 80 ka. Paleoceanography 10, 661–675.
Zühlsdorff, C., Wien, K., Stuut, J.-B. W., Henrich, R., 2007. Late Quaternary sedimentation within a submarine channel-levee system offshore Cap Timiris. Mauritania. Marine Geology 240, 217–234.